*J. Fluid Mech.* (1984), *vol.* 149, *pp.* 15–31
*Printed in Great Britain*



# Resonantly forced surface waves in a circular cylinder

By JOHN W. MILES

Institute of Geophysics and Planetary Physics, University of California, San Diego, La Jolla, CA 92093

(Received 14 May 1984)

The weakly nonlinear, weakly damped response of the free surface of a liquid in a vertical circular cylinder that is subjected to a simple harmonic, horizontal translation is examined by extending the corresponding analysis for free oscillations. The problem is characterized by three parameters, $\alpha$, $\beta$ and $d/a$, which measure damping, frequency offset (driving frequency − natural frequency), and depth/radius. The asymptotic ($t \uparrow \infty$) response may be any of: (i) harmonic (at the driving frequency) with a nodal line transverse to the plane of excitation (*planar* harmonic); (ii) harmonic with a rotating nodal line (*non-planar* harmonic); (iii) a periodically modulated sinusoid (limit cycle); (iv) a chaotically modulated sinusoid. It appears, from numerical integration of the evolution equations, that only motions of type (i) and (ii) are possible if $0.30 < d/a < 0.50$, but that motions of type (iii) and (iv) are possible for all other $d/a$ in some interval (or intervals) of $\beta$ if $\alpha$ is sufficiently small. Only motion of type (i) is possible if $\alpha$ exceeds a critical value that depends on $d/a$.

## 1. Introduction

The weakly nonlinear, resonant response (sloshing) of the free surface of water in a vertical, circular cylinder that is subjected to a simple harmonic, horizontal translation has been investigated by Hutton (1963). He concluded from his analysis that, as in the analogous problem for the spherical pendulum (Miles 1962): (*a*) harmonic† motion of the dominant mode with a nodal line perpendicular to the plane of excitation (cf. planar motion of the pendulum) is unstable in a certain neighbourhood of the natural frequency of that mode; (*b*) (nonlinearly) coupled motion of the two dominant modes with orthogonal nodal lines (cf. non-planar motion of the pendulum) is stable in a spectral neighbourhood that overlaps neighbourhoods of both stable and unstable motions of type (*a*); (*c*) no stable, harmonic motion is possible in a finite neighbourhood of the natural frequency. He confirmed these predictions in laboratory experiments.

I recently (Miles 1984*a*) reexamined the pendulum problem in order to explore the transitions from regular to chaotic motion in the context of *strange attractors*, which were discovered by Lorenz (1963) at about the time the above work was carried out and have since been widely investigated (for references see Lichtenberg & Lieberman 1983). This, in turn, led me to reexamine the fluid-sloshing problem, with the primary aims of introducing damping and determining the parametric regime (if any) in which chaotic motion is possible and the secondary aim of rendering Hutton's formulation both more compact and more flexible.

† I use 'harmonic' to mean *simple harmonic* or, equivalently, *monochromatic*.

I begin, in §2, by calculating the Lagrangian for the free-surface motion in the circular basin, using the amplitudes of the normal modes as generalized coordinates. This calculation follows an earlier formulation for nonlinear waves in cylinders of arbitrary cross-section (Miles 1976) and the specific application of that formulation to free, internally resonant oscillations in a circular cylinder (Miles 1984*b*); equations from these two papers are cited by the respective prefixes I and II. The non-axisymmetric normal modes for the circular basin occur in pairs, the members of which have the same radial and azimuthal wavenumbers, and therefore the same natural frequency, and differ only in the positions of their radial nodal lines; in particular, the dominant pair (azimuthal wavenumber one and no circumferential nodal lines) has nodal lines that may be chosen perpendicular and parallel, respectively, to the plane of excitation. The fluid motion is excited by a planar displacement $x_0 \cos \omega t$, where $x_0/a \equiv O(\epsilon^3)$, $0 < \epsilon \ll 1$, $a$ is the radius of the basin, $\omega - \omega_1 = O(\epsilon^2 \omega_1)$, and $\omega_1$ is the natural frequency of the dominant mode(s). This proximity to resonance implies the failure of the linear approximation; however, a uniformly valid approximation may be obtained by retaining terms of fourth order (in the amplitude) in the Lagrangian, which imply cubic nonlinearity in the equations of motion. The resonant balance between the inertial and gravitational restoring forces for the dominant modes implies a balance between the cubic and forcing terms, in consequence of which the amplitudes of the dominant modes are $O(\epsilon)$. Secondary modes of azimuthal wavenumbers 0 and 2 and amplitudes $O(\epsilon^2)$ are excited at frequencies of 0 and $2\omega$ through nonlinear coupling, as in II. The remaining modes are excited only at $O(\epsilon^3)$, except in small neighbourhoods of internal resonance (see §3), only one of which appears to be of practical importance. (It perhaps should be emphasized that the modal truncation in the present problem is fully justified by the restriction to resonant excitation and differs qualitatively from that invoked in Lorenz's (1963) model of convection.)

In §3 I pose the generalized coordinates of the dominant modes, say $\eta_1$ and $\eta_2$, as slowly modulated sinusoids with carrier frequency $\omega$ (the Van der Pol transformation) and those of the secondary modes as sinusoids with frequency $2\omega$ plus steady components, average the Lagrangian over the period $2\pi/\omega$ to eliminate the carrier, and then invoke Hamilton's principle and eliminate the amplitudes of the secondary modes to obtain (in §4) four, first-order, evolution equations for the four, slowly varying, amplitudes of the dominant modes. I also introduce linear damping at this point. These evolution equations comprise three parameters: $\alpha$, which measures damping; $\beta$, which measures resonant offset; and the aspect ratio $d/a$ ($d$ is the quiescent depth of the fluid). They are identical in form with the corresponding evolution equations for either the spherical pendulum (Miles 1984*a*) or a stretched string (Miles 1984*c*), but with coefficients that depend on the additional parameter $d/a$.

The analysis in §§5 and 6, wherein the equilibrium (*fixed*) and bifurcation points of the evolution equations and the stability of the equilibrium points are calculated, follows that for the pendulum. Numerical integrations, using the same programs (modified to incorporate the additional parameter $d/a$) as in the pendulum problem, yield similar phase-plane trajectories and power spectra. In particular, the asymptotic ($t \to \infty$) motion typically is harmonic if the evolution equations have a stable fixed point for a given set of parameters. This motion may be either planar or non-planar, depending on the fixed point; two stable fixed points, one corresponding to planar motion and the other to non-planar motion, exist in certain parametric regimes, and which motion is attained depends on the initial conditions. The motion is either a

periodically modulated sinusoid (limit cycle) or a chaotically modulated sinusoid in those parametric domains in which no stable fixed points exist. There is a limited domain, $0.30 < d/a < 0.50$, in which at least one stable fixed point exists, and limit cycles and chaotic motion are not found, for any combination of $\alpha$ and $\beta$; outside of this domain, limit cycles or chaotic motions are possible in some interval of $\beta$ if $\alpha$ is inferior to a critical value that depends on $d/a$.

## 2. The Lagrangian

We pose the free-surface displacement in the form

$$\eta(r,\theta,t) = \eta_n(t)\,\psi_n(r,\theta), \tag{2.1}$$

where $r$ and $\theta$ are plane polar coordinates, the repeated indices are summed over the participating modes, the $\eta_n$ are generalized coordinates,

$$\psi_n \equiv \psi_{ij}^{\mathrm{c,s}} = N_{ij}^{-1} J_i(k_{ij} r)\,(\cos i\theta,\ \sin i\theta) \quad (i = 0, 1, \ldots,\ j = 1, 2, \ldots), \tag{2.2a}$$

$$J_i'(k_{ij} a) = 0, \quad N_{ij}^2 = \tfrac{1}{2}(1+\delta_{0i})\left\{1-\left(\frac{i}{k_{ij}a}\right)^2\right\} J_i^2(k_{ij} a), \tag{2.2b,c}$$

where $J_i$ is a Bessel function, and $k_{ij}$ is one of the infinite, discrete set of eigenvalues determined by (2.2*b*);

$$\int_0^a \int_0^{2\pi} \psi_m \psi_n\, r\,\mathrm{d}r\,\mathrm{d}\theta = \delta_{mn}\,\pi a^2, \tag{2.3}$$

where $\delta_{mn}$ is the Kronecker delta. Each of the eigenfunctions requires three indices (the azimuthal wavenumber $i$, the radial wavenumber $j$, and, except for the axisymmetric modes, the superscript c or s to distinguish between cosine and sine azimuthal variations) for its complete specification, and the use of a single index in (2.1) and subsequently is merely a convenient abbreviation. We reserve the single subscripts 1 and 2 for the dominant (or primary) modes according to

$$\psi_{1,2} \equiv \psi_{11}^{\mathrm{c,s}} = N^{-1} J_1(kr)\,(\cos\theta,\ \sin\theta) \quad (N \equiv N_{11} = 0.3455,\ \ k \equiv k_{11} = 1.8412/a). \tag{2.4}$$

The Lagrangian for free oscillations is given by II(2.12). In the present problem, in which the basin is subjected to the $x$-directed displacement $x_0 \cos\omega t$, II(2.12) must be augmented by the external potential $-F_1\eta_1$, where

$$F_1 = -\ddot{x}_0 x_1 = \omega^2 x_0 x_1 \tag{2.5}$$

is the generalized force obtained by letting $\dot{\boldsymbol{u}}\cdot\boldsymbol{x} = \ddot{x}_0 x_1$ in I (3.5*a*), and

$$x_1 = (\pi a^2)^{-1} \int_0^a \int_0^{2\pi} x\psi_1\, r\,\mathrm{d}r\,\mathrm{d}\theta = 0.4968a \tag{2.6}$$

is derived from I(3.5*b*).† The end result is

$$L \equiv T - V = F_1\eta_1 + \tfrac{1}{2}a_n(\dot{\eta}_n^2 - \omega_n^2\eta_n^2) + \tfrac{1}{2}a_{lmn}\eta_l\dot{\eta}_m\dot{\eta}_n + \tfrac{1}{4}a_{jlmn}\eta_j\eta_l\dot{\eta}_m\dot{\eta}_n, \tag{2.7}$$

wherein terms of sixth order in $\eta_n$ have been neglected,

$$a_n = k_n^{-1}\coth k_n d \equiv g/\omega_n^2, \tag{2.8}$$

† The generalized forces also are non-zero for, and therefore excite, each of the remaining $\psi_{ij}^{\mathrm{c}}$ modes; however, the amplitudes of these modes are $O(\epsilon^3)$ and therefore negligible compared with those, (3.1) and (3.2), included in the present formulation.

$\omega_n$ is the natural frequency (so that $a_n$ is the equivalent pendulum length) of the $n$th mode, and the coefficients $a_{lmn}$ (dimensionless) and $a_{jlmn}$ (inverse length) are defined by I(3.3) and calculated in the appendix of II.

## 3. The average Lagrangian

The equations of motion implied by (2.7) contain terms of first and third order in the dominant modes, $\eta_{1,2}$. The linear inertial and gravitational restoring terms in the equations for the dominant modes approximately cancel in the neighbourhood of resonance ($\omega \approx \omega_1$), and a balance between the nonlinear terms and $F_1 = O(\epsilon^3)$, where $\epsilon$ is a dimensionless scaling parameter (see (3.5) below), implies $\eta_{1,2} = O(\epsilon)$. Secondary (non-resonant) modes are forced by terms that are quadratic in $\eta_1$ and $\eta_2$ and therefore are $O(\epsilon^2)$. A consistent formulation then requires that each of the four terms in the brackets in (2.7) be $O(\epsilon^4)$. It follows that the resonant neighbourhood is defined by $\omega^2 - \omega_1^2 = O(\epsilon^2\omega^2)$. It also follows that (as in II) two of the terms in the triple product $\eta_l \dot{\eta}_m \dot{\eta}_n$ must correspond to the dominant modes, and $a_{lmn}$ then differs from zero only if the third term corresponds to a secondary mode with azimuthal wavenumber 0 or 2 (the products of the dominant modes introduce $\sin^2\theta$, $\cos^2\theta$ and $\sin 2\theta$ in the correlation integrals from which $a_{lmn}$ is derived, and these products are orthogonal to $\cos i\theta$ and $\sin i\theta$ unless $i = 0$ or 2). The dominant modes may be posed as slowly varying sinusoids with the carrier frequency $\omega$; accordingly, the quadratically forced secondary modes must have carrier frequencies of 0 or $2\omega$. Guided by these considerations, we posit

$$\eta_n = \epsilon\lambda\{p_n(\tau)\cos\omega t + q_n(\tau)\sin\omega t\} \quad (n = 1, 2) \tag{3.1}$$

for the dominant modes and

$$\eta_n = \epsilon^2\lambda\{A_n(\tau)\cos 2\omega t + B_n(\tau)\sin 2\omega t + C_n(\tau)\} \quad (n \neq 1, 2) \tag{3.2}$$

for the secondary modes, where

$$\lambda = k^{-1}\tanh kd \tag{3.3}$$

is a reference length, $p_n$, $q_n$, $A_n$, $B_n$ and $C_n$ are slowly varying, dimensionless amplitudes, and

$$\tau = \tfrac{1}{2}\epsilon^2\omega t \tag{3.4}$$

is a dimensionless slow time.

We now substitute (3.1) and (3.2) into (2.7) and average $L$ over a $2\pi$ interval of $\omega t$ while holding $\tau$ fixed (this average is denoted by $\langle\ \rangle$). Proceeding as in II§3 (the present calculation of $\langle L\rangle$ differs from that in II only in the addition of the forcing term $F_1\eta_1$ and in the choice of $\omega$, rather than $\omega_1$, as the carrier frequency), we find that $A_n$, $B_n$ and $C_n$ are given by II(3.10). Substituting these results into $\langle L\rangle$ and choosing

$$\epsilon^3 = \frac{x_0 x_1}{a_1\lambda} = k^2 x_0 x_1, \tag{3.5}$$

we obtain (cf. II(3.11))

$$\langle L\rangle = \tfrac{1}{2}\epsilon^4 g\lambda^2\{\tfrac{1}{2}(\dot{p}_n q_n - p_n\dot{q}_n) + H(p_1, q_1, p_2, q_2)\}, \tag{3.6}$$

wherein $n$ is summed over 1, 2, an error factor of $1 + O(\epsilon^2)$ is implicit,

$$H = p_1 + \beta E + \tfrac{1}{2}AE^2 + \tfrac{1}{2}BM^2, \tag{3.7}$$

$$\beta = \frac{\omega^2 - \omega_1^2}{\epsilon^2\omega_1^2} \equiv A^{\frac{1}{3}}\bar{\beta}, \tag{3.8}$$

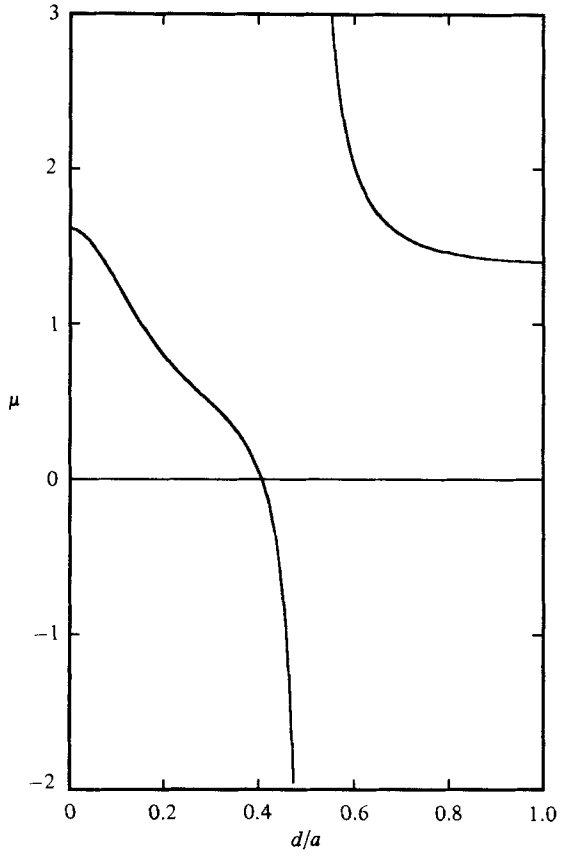


FIGURE 1. The parameter $\mu$, as defined by (3.11) and calculated from the results in II (Appendix). The pole at $d/a = 0.5059$ reflects the corresponding zero of $A$.

$$E = E_1 + E_2, \quad E_n = \tfrac{1}{2}(p_n^2 + q_n^2), \tag{3.9a,b}$$

$$M = p_1 q_2 - p_2 q_1 \tag{3.10}$$

($E$ and $M$ are measures of the energy and the angular momentum in the dominant modes), and $A$ and $B$, which depend only on the aspect ratio $d/a$, are given by II (A 23) and are plotted in figures II 1–3. The tuning parameter $\beta$ measures the frequency offset ($\beta \equiv 0$ in II); the weak ($\epsilon \ll 1$) nonlinearity considered here is negligible if $|\beta| \gg 1$. The rescaled frequency parameter $\bar{\beta}$ proves to be convenient for numerical plots.

Both $A$ and $B$ have simple poles at $d/a = 0.1523$ in consequence of the internal resonance between the primary modes ($ka = 1.8412$) and the dominant axisymmetric mode ($k_{01}a = 3.8317$), and the present formulation fails in some neighbourhood of this resonance (there also are internal resonances with the 02 and 22 modes, but they are extremely narrow; see II). It is due in part to these poles and in part to the zeros of $A$ and $B$ at $d/a = 0.5059$ and 0.4063 respectively, that we choose not to absorb either $A$ or $B$ in $\lambda$. The advantages of such a re-scaling are, in any event, minor, since both $A$ and $B$ are determined by the single parameter $d/a$. We also find it convenient to introduce

$$\mu = -B/A, \tag{3.11}$$

which is plotted in figure 1. Note that $\mu$ does *not* have a pole at $d/a = 0.1523$ and is positive except in the domain (bounded by the zeros of $A$ and $B$)

$0.406 < d/a < 0.506$. It seems likely that higher-order terms would need to be incorporated in the Lagrangian to obtain results that are uniformly valid near either $A$ or $B = 0$; however, since nonlinearity is weak in these neighbourhoods, and since the corresponding range of $d/a$ is small, I have not examined this question in detail.

## 4. Evolution equations

Requiring $\langle L \rangle$ (3.6) to be stationary with respect to each of the $p_n$ and $q_n$, we obtain the canonical equations

$$\dot{p}_n = -\frac{\partial H}{\partial q_n}, \quad \dot{q}_n = \frac{\partial H}{\partial p_n}, \tag{4.1a,b}$$

in which $H$ now appears as a Hamiltonian (which would be a constant of the motion in the absence of damping). Linear damping may be incorporated at this stage by adding the terms $-\alpha(p_n, q_n)$ to the right-hand side of (4.1$a,b$), where

$$\alpha = 2\delta/\epsilon^2 \tag{4.2}$$

and $\delta$ is the damping ratio ($2\pi\delta$ is the logarithmic decrement) of free oscillations in the dominant mode.† Substituting (3.7) into (4.1) and incorporating damping, we obtain

$$\dot{p}_1 = -\alpha p_1 - (\beta + AE) q_1 + BMp_2, \quad \dot{q}_1 = -\alpha q_1 + (\beta + AE) p_1 + BMq_2 + 1, \tag{4.3a,b}$$

$$\dot{p}_2 = -\alpha p_2 - (\beta + AE) q_2 - BMp_1, \quad \dot{q}_2 = -\alpha q_2 + (\beta + AE) p_2 - BMq_1. \tag{4.3c,d}$$

Note that (4.3) are invariant under the reflection $(p_2, q_2) \rightarrow -(p_2, q_2)$ by virtue of symmetry with respect to the plane of excitation ($\theta = 0$).

The evolution equations (4.3) reduce to the corresponding equations for a spherical pendulum (Miles 1984$a$) if $A = \frac{1}{4}$ and $B = -\frac{3}{4}$ ($\mu = 3$, which is realized in the present context only if $d/a$ is rather close to the zero of $A$). They reduce to the corresponding equations for a resonantly forced string (Miles 1984$c$) if $A = -3$ and $B = 1$ ($\mu = \frac{1}{3}$). The response of the pendulum is chaotic in various intervals of $\beta$ if $\alpha$ is sufficiently small, whereas the response of the string appears (on the basis of numerical results) to be regular for all $\alpha$ and $\beta$.

The divergence of the set (4.3) in the $(p_1, p_2, q_1, q_2)$-space is

$$\Delta \equiv \frac{\partial \dot{p}_1}{\partial p_1} + \frac{\partial \dot{q}_1}{\partial q_1} + \frac{\partial \dot{p}_2}{\partial p_2} + \frac{\partial \dot{q}_2}{\partial q_2} = -4\alpha. \tag{4.4}$$

It follows that an element of volume in this space contracts like $\exp(-4\alpha\tau)$, and every trajectory ultimately must be confined to a limiting subspace of dimension less than four, which may be a fixed point (dimension zero), a closed curve (dimension one), a torus (dimension two or three), or a strange attractor (fractional dimension). It also may be shown that every trajectory ultimately must lie within the hypersphere $E \leqslant 1/2\alpha^2$ (cf. Miles 1984$a$).

† Linear damping could have been included in the initial formulation to obtain the same end results, but then the average Lagrangian could not have been introduced, and the resulting derivation of (4.3) would have been much longer. That linear damping must contribute the terms $-\alpha p_1, \ldots$ in (4.3) may be confirmed by neglecting the nonlinear terms therein and solving the resulting equations to obtain the linear approximation to the envelope of the sinusoidal carrier.

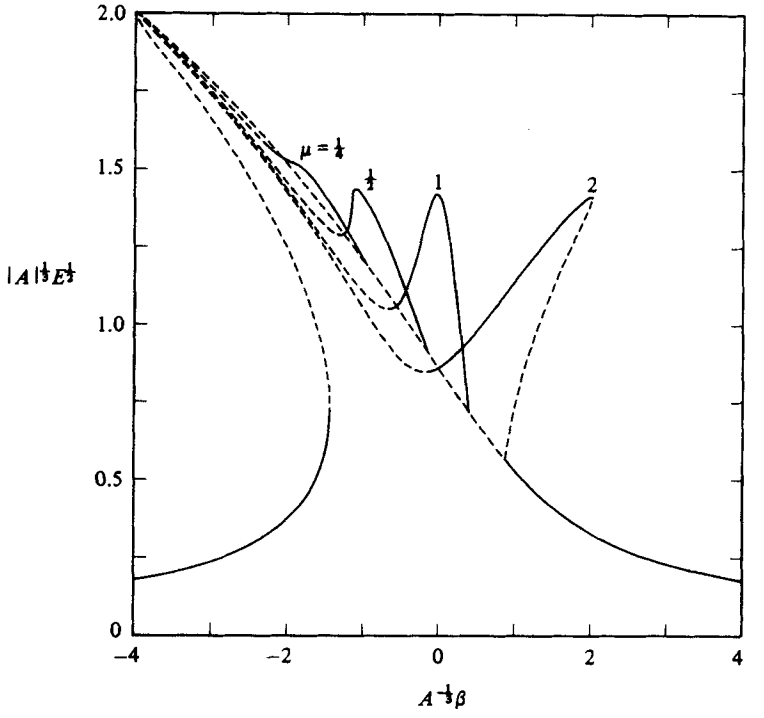


FIGURE 2. The resonance curves for $A^{-\frac{1}{3}}\alpha^2 = \frac{1}{8}$ and $\mu = \frac{1}{4}$, $\frac{1}{2}$, 1 and 2. The dashed portions of the curves correspond to unstable fixed points (the fixed points on the planar resonance curve are unstable between the termini ($\beta_2$ and $\beta_4$) of the non-planar curve). The bifurcation points $\beta_1$, $\beta_2$ and $\beta_{1*}$ are not resolved on the scale of the drawing.

## 5. Fixed points

The fixed points of (4.3), as obtained by setting $\dot{p}_n = \dot{q}_n = 0$ and solving the resulting algebraic equations for $p_n$ and $q_n$, are given by

$$p_1 = -2(\beta E + AE^2 + BM^2), \quad q_1 = 2\alpha E, \tag{5.1a,b}$$

$$p_2 = -2\alpha M, \quad q_2 = -2\{\beta + (A+B)E\}M, \tag{5.1c,d}$$

where either $BM = 0$ and

$$A^2E^3 + 2A\beta E^2 + (\alpha^2+\beta^2)E - \tfrac{1}{2} = 0 \quad (BM = 0) \tag{5.2}$$

for planar ($p_2 = q_2 = 0$) motion† or

$$B^2M^2 = -(AE+\beta)\{(A+2B)E+\beta\} - \alpha^2 > 0 \tag{5.3}$$

and

$$A(A+B)^2E^3 + (A+B)(3A+B)\beta E^2 + \{A\alpha^2 + (3A+2B)\beta^2\}E + \beta(\alpha^2+\beta^2) + \tfrac{1}{4}B = 0 \tag{5.4}$$

for non-planar motion. Only the positive-real roots of (5.2) and those positive-real roots of (5.4) for which $M^2 > 0$ are physically significant.

† Following the terminology for the pendulum, I use *planar* to describe those motions for which $p_2 = q_2 = 0$. In the present context, this implies that the maximum free-surface displacement is in the plane of excitation.

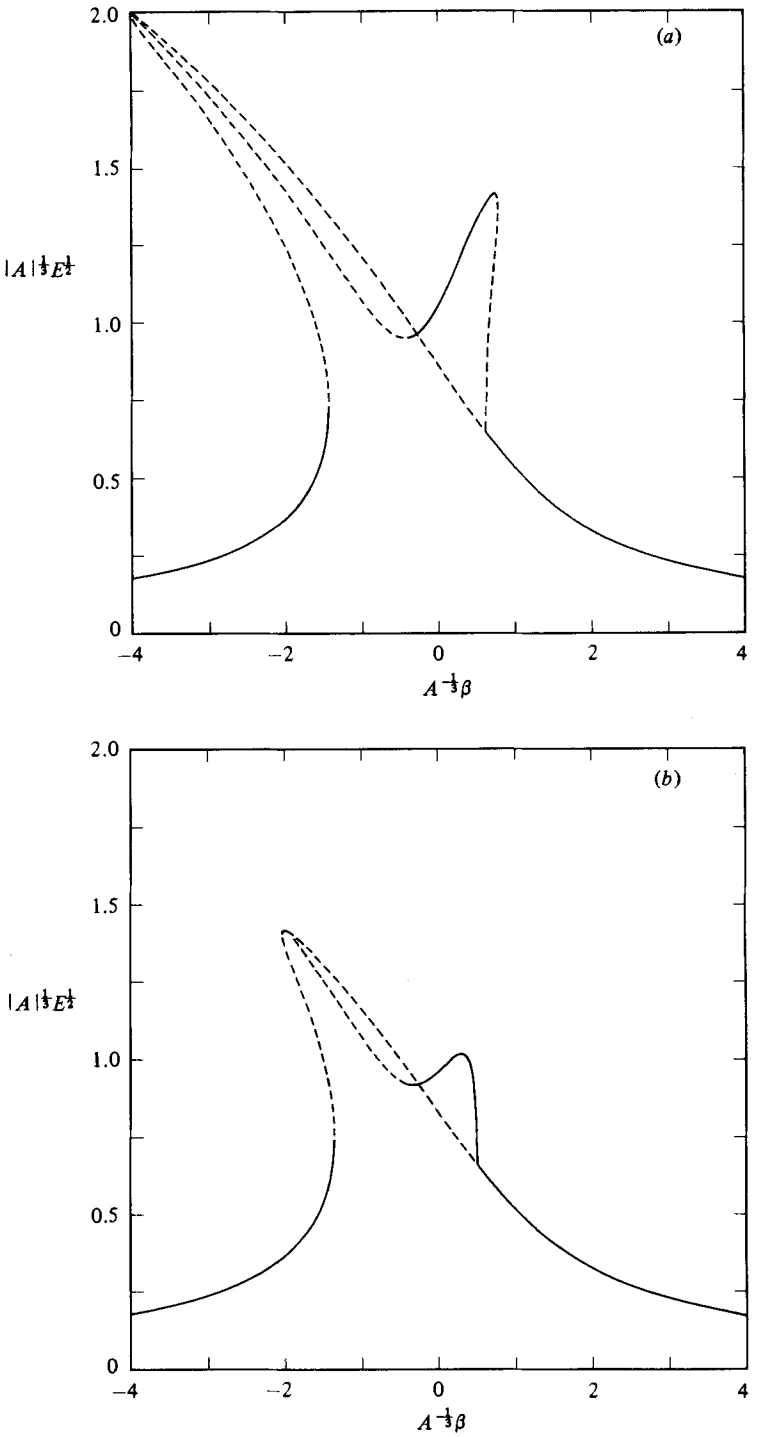


FIGURE 3. The resonance curves for $\mu = 1.377$ and $A^{-\frac{2}{3}}\alpha^2 = \frac{1}{8}$ (*a*), $\frac{1}{4}$ (*b*), $\frac{3}{8}$ (*c*). There are no Hopf-bifurcation points for $A^{-\frac{2}{3}}\alpha^2 = \frac{3}{8}$.

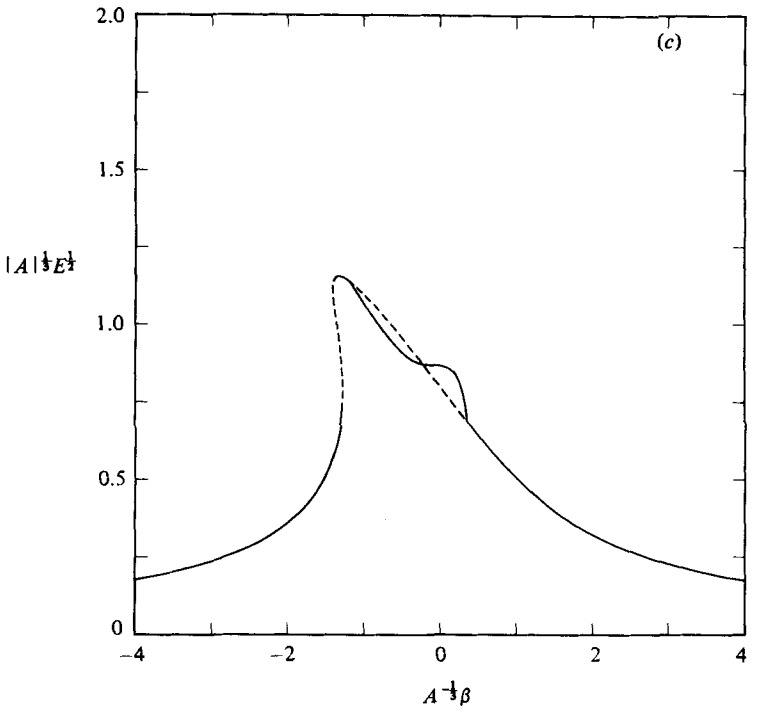


FIGURE 3(*c*). For caption see opposite page.

We now examine the resonance curves, $E$ versus $\beta$ with $\alpha$ and $d/a$ as family parameters, and their Poincaré-bifurcation points. (I have used the modifier 'Poincaré' in the sense of Gurel (1979). The Hopf-bifurcation points are considered in §6.) Representative examples are plotted in the similarity form $|A|^{\frac{1}{3}}E^{\frac{1}{2}}$ versus $A^{-\frac{1}{3}}\beta = \bar{\beta}$ with $A^{-\frac{2}{3}}\alpha^2 = \frac{1}{8}$, which is representative of small $\alpha$ (the most interesting case), and various $\mu$ in figure 2 and for $\mu = 1.377$ ($d/a = \infty$) and various $\alpha^2$ in figure 3. (I have not presented results for $\mu < 0$ ($0.406 < d/a < 0.506$), both because their significance is questionable (see last sentence in §3) and because it appears that anharmonic motion is possible only in a small subinterval ($0.500 < d/a < 0.506$) of this interval (see last paragraph in §6).) The resonance curves become progressively simpler as $\alpha$ increases to $\alpha_* = 0.687|B|^{\frac{1}{3}}$ (see (5.12) below) and are of little interest in the present context if $\alpha > \alpha_*$; see Miles (1984*a*) for examples. The Poincaré-bifurcation points, at each of which there is a change in the number of fixed points, correspond to the turning points (at which $\mathrm{d}\beta/\mathrm{d}E = 0$) of the resonance curves and to the termini (at which $M^2 = 0$) of the non-planar resonance curves.

The planar resonance curve, which is determined by (5.2), is isomorphic to that for the pendulum. It has a maximum at

$$E = -A^{-1}\beta = \tfrac{1}{2}\alpha^{-2} \tag{5.5}$$

and corresponds to a 'soft'/'hard' spring (in the terminology of mechanics) for $A \gtrless 0$, although the planar resonance curve in figures 2 and 3 leans to the left for either sign of $A$ in consequence of the choice of $\bar{\beta}$ as the frequency parameter. The turning points

$\beta_1$ and $\beta_3$ (the indices correspond to those for the pendulum), at which $\bar{\beta}$ is a minimum and maximum respectively, are given by

$$\beta_1 = -\tfrac{1}{2}A\alpha^{-2} - \tfrac{1}{2}A^{-1}\alpha^4 + O(\alpha^{10}), \quad \beta_3 = -\tfrac{3}{2}A^{\frac{1}{3}} + \tfrac{1}{2}A^{-\frac{1}{3}}\alpha^2 + O(\alpha^4). \tag{5.6a,b}$$

They coincide at

$$\beta_1 = \beta_3 = -\tfrac{3}{2}(\tfrac{1}{2}A)^{\frac{1}{3}} \quad \text{for} \quad \alpha = \tfrac{1}{2}3^{\frac{1}{2}}\,|\tfrac{1}{2}A|^{\frac{1}{3}}, \tag{5.7a,b}$$

and the planar resonance curve is single-valued for $\alpha > 0.687|A|^{\frac{1}{3}}$.

The non-planar resonance curve, which is determined by (5.4) subject to the side condition (5.3), has a maximum at

$$E = \tfrac{1}{4}\alpha^{-2}, \quad \beta = -\tfrac{1}{4}(A+B)\,\alpha^{-2}. \tag{5.8a,b}$$

It terminates on the planar resonance curve at the bifurcation points $\beta_2$ and $\beta_4$, which are determined by the coincidence of the roots of $M^2(5.3) = 0$ and (5.2). Eliminating $\beta$ between these two equations, we obtain

$$E^3(1 - 2\alpha^2 E) = \tfrac{1}{8}B^{-2}, \tag{5.9}$$

which has two positive-real roots for sufficiently small $\alpha^2$. The corresponding bifurcation points are given by

$$\beta_n = -AE_n - \tfrac{1}{4}B^{-1}E_n^{-2} \quad (n = 2, 4), \tag{5.10}$$

wherein $E_{2(4)}$ is the larger (smaller) positive-real root of (5.9). Solving (5.9) and (5.10) for $\alpha^2 \ll 1$, we obtain

$$\beta_2 = -\tfrac{1}{2}A\alpha^{-2} + B^{-2}(\tfrac{1}{2}A - B)\,\alpha^4 + O(\alpha^{10}), \tag{5.11a}$$

$$\beta_4 = -B^{-\frac{2}{3}}(\tfrac{1}{2}A + B) - \tfrac{2}{3}B^{-\frac{4}{3}}(\tfrac{1}{4}A - B)\,\alpha^2 + O(\alpha^4). \tag{5.11b}$$

These two bifurcation points coincide at

$$\beta_2 = \beta_4 = -(4B)^{-\frac{2}{3}}(2A + B) \quad \text{for} \quad \alpha = \tfrac{1}{2}3^{\frac{1}{2}}\,|\tfrac{1}{2}B|^{\frac{1}{3}} \equiv \alpha_*; \tag{5.12a,b}$$

(5.9) has no positive-real roots, and the non-planar resonance curve disappears, for $\alpha > \alpha_*$. The bifurcation points $\beta_1$ and $\beta_2$ are unresolved on the scale of figure 2; however, it follows from (5.6$a$) and (5.11$a$) that $\beta_2 - \beta_1 > 0$ for $0 < \alpha^2 \ll 1$.

The cubic equation (5.4) has two turning points, $\beta_5$ and $\beta_6$, if

$$\alpha > \tfrac{1}{2}3^{\frac{1}{2}}\left|\frac{(A+B)\,B}{4A}\right|^{\frac{1}{3}}, \tag{5.13}$$

but either or both of $\beta_5$ and $\beta_6$ may be excluded as turning points of the non-planar resonance curve by the requirements $E > 0$ and $M^2 > 0$. Solving $\mathrm{d}\beta/\mathrm{d}E = 0$ for $\alpha^2 \ll 1$, we obtain

$$\beta_5 = -\tfrac{1}{4}(A+B)\,\alpha^{-2} - \left(\frac{A}{B}\right)^2 (A+B)^{-1}\,\alpha^4 + O(\alpha^{10}), \tag{5.14a}$$

$$\beta_6 = -3\left(\frac{A}{4B}\right)^{\frac{2}{3}}(A+B)^{\frac{1}{3}} + 2^{-\frac{2}{3}}\left(\frac{A}{B}\right)^{\frac{4}{3}}(A+B)^{-\frac{1}{3}}\,\alpha^2 + O(\alpha^4). \tag{5.14b}$$

It should be emphasized that each point on the non-planar resonance curve corresponds to a pair of equilibrium points, which are related through $(M, p_2, q_2) \to -(M, p_2, q_2)$ (see remark following (4.3)).

## 6. Stability of fixed points

Substituting

$$(p_i, q_i) = (p_i^0, q_i^0) + (P_i, Q_i)\,\mathrm{e}^{\sigma\tau}, \tag{6.1}$$

where $(p_i^0, q_i^0)$ are the coordinates of a particular fixed point and $|P_i|, |Q_i| \ll 1$, into (4.3), neglecting terms of second and third order in $P_i$ and $Q_i$, and requiring the determinant of the resulting linear equations in $P_i$ and $Q_i$ to vanish, we obtain

$$F(\sigma) = (\sigma+\alpha)^4 + 2D_2(\sigma+\alpha)^2 + D_0 = 0, \tag{6.2}$$

where

$$D_0 = \begin{vmatrix} \hat{\beta}+Ap_1^2+Bq_2^2 & Ap_1q_1-Bp_2q_2 & Ap_1p_2-Bq_1q_2 & Cp_1q_2-Bp_2q_1 \\ Ap_1q_1-Bp_2q_2 & \hat{\beta}+Aq_1^2+Bp_2^2 & Cp_2q_1-Bp_1q_2 & Aq_1q_2-Bp_1p_2 \\ Ap_1p_2-Bq_1q_2 & Cp_2q_1-Bp_1q_2 & \hat{\beta}+Ap_2^2+Bq_1^2 & Ap_2q_2-Bp_1q_1 \\ Cp_1q_2-Bp_2q_1 & Aq_1q_2-Bp_1p_2 & Ap_2q_2-Bp_1q_1 & \hat{\beta}+Aq_2^2+Bp_1^2 \end{vmatrix}, \tag{6.3a}$$

$$(p_i, q_i) \equiv (p_i^0, q_i^0), \quad \hat{\beta} = \beta + AE, \quad C = A+2B, \tag{6.3b,c,d}$$

$$D_2 = \hat{\beta}^2 + (A+B)\hat{\beta}E + BCM^2. \tag{6.4}$$

The necessary and sufficient conditions for the real parts of the roots of the quartic equation (6.2) to be non-positive – i.e. for the perturbation (6.1) be stable – are

$$F(0) = \alpha^4 + 2D_2\alpha^2 + D_0 \geqslant 0, \tag{6.5a}$$

$$D_2 + \alpha^2 \geqslant 0, \quad (D_2+2\alpha^2)^2 - D_0 \geqslant 0. \tag{6.5b,c}$$

The discriminant $F(0)$ vanishes at the turning points ($\beta = \beta_{1,3,5,6}$) of the planar and non-planar resonance curves and at their intersections ($\beta = \beta_{2,4}$), i.e. at the Poincaré-bifurcation points. It is negative ($\mathrm{Re}\,\sigma > 0$) on the intermediate branch of the planar resonance curve ($\bar{\beta}_1 < \bar{\beta} < \bar{\beta}_3$) if that branch exists ($\alpha < 0.687|A|^{\frac{1}{3}}$) and on that portion intercepted by the non-planar resonance curve ($\alpha < 0.687|B|^{\frac{1}{3}}$, $\bar{\beta}_2 < \bar{\beta} < \bar{\beta}_4$). It also is negative on the intermediate branch of the non-planar resonance curve if that curve has three branches (as for $\mu < 0$) or on the lower branch where two branches exist (e.g. $\mu = 2$ in figure 2).

The zeros of the discriminant (6.5*c*), $\beta_{1*}$ and $\beta_{2*}$, are Hopf-bifurcation points, at which the real parts of a pair of complex-conjugate zeros of $F(\sigma)$ become positive. Numerical values for $A^{-\frac{2}{3}}\alpha^2 = \frac{1}{8}$ are plotted in figure 4. It may be established analytically that (cf. (5.6*a*) and (5.11*a*))

$$\beta_{1*} = -\tfrac{1}{2}A\alpha^{-2} + O(\alpha^4) \tag{6.6}$$

as $\alpha \downarrow 0$, and it follows from the numerical results that $\bar{\beta}_{1*} > \bar{\beta}_2$. If $\alpha$ is sufficiently small and $\mu$ is sufficiently large, $\bar{\beta}_{2*} > \bar{\beta}_3$, and there is a finite range, $\bar{\beta}_3 < \bar{\beta} < \bar{\beta}_{2*}$, in which neither planar nor non-planar harmonic motion is stable; but if $-1 < \mu < \mu_c$, where $\mu_c$ is slightly less than 0.50, $\bar{\beta}_{2*} < \bar{\beta}_3$ (if $\alpha$ is sufficiently small for $\beta_{2*}$ to exist), and either planar or non-planar harmonic motion is stable for all $\beta$. It then appears that limit cycles and/or chaotic motions are impossible for $0.30 < d/a < 0.50$.

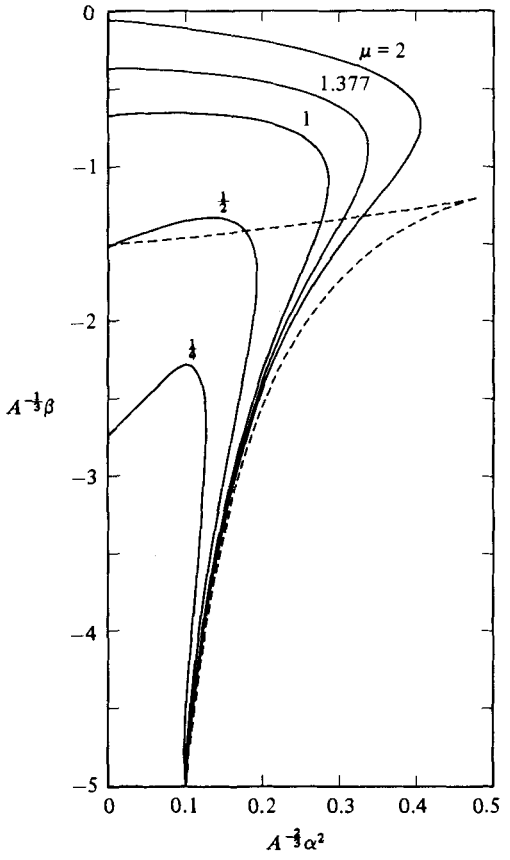


FIGURE 4. The Hopf-bifurcation points, $\bar{\beta}_{1,2*}$ ($\bar{\beta}_{1*} < \bar{\beta}_{2*}$) for $\mu = \frac{1}{4}, \frac{1}{2}$, 1, 1.377 and 2 (——) and the turning points, $\bar{\beta}_{1,3}$ ($\bar{\beta}_1 < \bar{\beta}_3$) of the planar resonance curve (----).

## 7. Asymptotic trajectories

The asymptotic (i.e. attained after the decay of transients) phase-space trajectory depends on $\alpha$, $\beta$ and $\mu$ and, in a more limited sense, the initial conditions. Numerical integrations suggest that, at least if the Hopf bifurcations are supercritical (as they appear to be in the present problem), a trajectory terminates on a stable fixed point if at least one exists for the prescribed $\alpha$ and $\beta$; if there are more than one (either two or three in the present context) such points, which is attained depends on the initial conditions. The asymptotic trajectories in those parametric domains in which no stable equilibrium points exist ($\bar{\beta}_3 < \bar{\beta} < \bar{\beta}_{2*}$) are non-planar and either periodic or chaotic.† The periodic trajectories are limit cycles and are uniquely determined by $\alpha$, $\beta$ and $\mu$ up to the reflection $(p_2, q_2) \rightarrow -(p_2, q_2)$, and which of a complementary pair is realized depends on the initial conditions; e.g. the limit cycle obtained for the initial conditions $(p_1, q_1, p_2, q_2) = (0, 0, 0, 1)$ is replaced by its complement if the initial conditions are replaced by $(0, 0, 0, -1)$.

† It follows from the Poincaré–Bendixson theorem and (4.4) that a *planar* trajectory must be asymptotic to a stable fixed point if one exists. The non-planar motions conceivably could be quasi-periodic (comprising two or more incommensurate frequencies), but no such asymptotic trajectories were obtained in the parametric domains that were numerically explored.

Periodic solutions of (4.3) presumably could be obtained by positing Fourier series and regarding the fundamental frequency as an eigenvalue; however, the algebra is forbidding. The angular frequency (for the slow time $\tau$) in the limit $\beta \uparrow \beta_{2*}$ (we anticipate that the Hopf bifurcation at $\beta = \beta_{2*}$ is supercritical, so that the periodic solution is stable), as obtained by setting $\sigma = \mathrm{i}\omega_*$ in (6.2) and requiring the imaginary part of the result to vanish (the vanishing of the real part is equivalent to the vanishing of the left-hand side of (6.6*c*)), is given by

$$\omega_*^2 = \alpha^2 + D_2. \tag{7.1}$$

(The second pair of eigenvalues for $\beta = \beta_{2*}$ is given by $\sigma = -2\alpha \pm \mathrm{i}\omega_*$.)

Chaotic solutions presumably are sensitive to small changes in the numerical specifications of $\alpha$, $\beta$, $\mu$ and the initial conditions. Nevertheless, their general appearance (or at least that of their $(p_1, p_2)$-projections) does appear to be determined for specified $\alpha$, $\beta$ and $\mu$ to within a possible mixing of a complementary pair of trajectories that are related through the reflection $(p_2, q_2) \rightarrow -(p_2, q_2)$; see below.

## 8. Numerical integrations

Numerical integrations of (4.3) were carried out using an Adams–Bashforth routine with a round-off error of less than $10^{-4}$. (Decreasing the round-off error from $10^{-4}$ to $10^{-6}$ made no perceptible difference in a subset of the results presented here.) Various plane projections ($(p_1, p_2)$, $(q_1, q_2)$, $(p_1, q_1)$, $(p_2, q_2)$) and Poincaré sections of the phase-space trajectories had been examined in the pendulum problem ($\mu = 3$) and led to the decision that the $(p_1, p_2)$-projections offered the optimum combination of information and computing economy. These projections are Poincaré maps of the $(\eta_1, \eta_2)$-projections of the free-surface displacement at the periodically spaced instants $\omega t = 0 \pmod{2\pi}$.

The power spectra of $N$-point runs of $E$ were determined through a fast-Fourier-transform routine according to

$$P(f_k) = \frac{2\Delta}{N} \left| \sum_{n=0}^{N-1} E(\tau_n)\, w(\tau_n) \exp(-2\pi \mathrm{i} f_k \tau_n) \right|^2, \tag{8.1}$$

where

$$f_k = \frac{k}{T}, \quad \tau_n = n\Delta \tag{8.2a,b}$$

are the discrete, dimensionless frequency and time, $\Delta$ is the increment of $\tau$, $T \equiv N\Delta$ is the length of the run ($0 < \tau < T$), and

$$w(\tau) = (\tfrac{2}{3})^{\frac{1}{2}} \left[ 1 - \cos \frac{2\pi\tau}{T} \right] = (\tfrac{8}{3})^{\frac{1}{2}} \sin^2 \frac{\pi\tau}{T} \tag{8.3}$$

is the window (or taper) function, normalized to an r.m.s. value of unity. The value of $\Delta$ for all runs was $2^{-4}$. The corresponding Nyquist frequency, 16, is roughly two orders of magnitude above the fundamental frequency $f_1$ or spectral peak in the following results. Numerical noise was below $P = 10^{-8}$. The zero-frequency components of the power spectra in figure 5 have been eliminated by omitting the first two ($k = 0, 1$) terms.

Both the $(p_1, p_2)$-trajectories and the power spectra in those parametric ranges that were sampled and for which $\bar{\beta}_{2*} > \bar{\beta}_3$ (so that either limit cycles or chaotic motion may occur) resemble those for the resonant forcing of a spherical pendulum (Miles 1984*a*); accordingly, only a few results are presented here. The results for $\mu = 1.3772$

| $\bar{\beta} = A^{-\frac{1}{3}}\beta$ | $\log_2 T$ | Trajectory |
|---|---|---|
| 0.8 (−0.2) −0.2 | 5 | FP† |
| −0.4 | 6 | Weak LC |
| −0.5 | 6 | Weak LC |
| −0.52 | 10 | LC (figure 5*a*) |
| −0.53 | 8 | LC–weak PD |
| −0.54 | 10 | LC–PD (figure 5*b*) |
| −0.56, −0.58, −0.60 | 7 | LC–PD |
| −0.70 | 10 | Chaotic + periodic (figure 5*c*) |
| −0.80 | 7 | Chaotic |
| −0.85 | 10 | Chaotic (figure 5*d*) |
| −0.90 | 7 | Chaotic |
| −1.43 | 7 | Chaotic |
| −1.44 | 6 | FP |

† FP ≡ fixed point, LC ≡ limit cycle, PD ≡ period doubling.

TABLE 1. Results of numerical integration for $\mu = 1.3772$, $A^{-\frac{2}{3}}\alpha^2 = \frac{1}{8}$

and $\alpha^2 = \frac{1}{8}A^{\frac{2}{3}}$, with $\bar{\beta}$ decreasing from values above $\bar{\beta}_{2*} = -0.400$ to values below $\bar{\beta}_3 = -1.44$, are described in table 1 and plotted in figure 5. Trajectories for $\bar{\beta} > -0.40$ spiral into the calculated fixed points, although rather slowly as $\bar{\beta} \downarrow -0.40$. A limit cycle, which projects as an oval in the $(p_1, p_2)$-plane, appears at $\bar{\beta} = -0.40$ and increases in amplitude as $\bar{\beta}$ is decreased below this value. The fundamental frequencies of the damped oscillations for $\bar{\beta}$ just above $-0.40$ and of the limit cycles for $\bar{\beta}$ just below $-0.40$ approximate $f_*$, as calculated from (7.1). A typical limit cycle, $\bar{\beta} = -0.52$, is displayed in figure 5(*a*). Weak period doubling appears at $\bar{\beta} = -0.53$ and persists at least down to $\bar{\beta} = -0.60$; see e.g. figure 5(*b*). It is to be expected that a more careful search would produce transitions to period quadrupling, octupling, etc. (as in the pendulum problem) before the transition to chaotic motion. Chaos appears at $\beta = -0.70$ (figure 5*c*), for which the power spectrum contains both broadband components and lines corresponding to a dominant frequency (the descendant of $f_*$) and its integral and half-order subharmonics. The corresponding $(p_1, p_2)$-trajectory is built up from a sequence of double-period trajectories such as that for $\bar{\beta} = -0.54$, but with each complete cycle displaced from the preceding cycle. It seems likely that this trajectory ultimately would fill a finite area in the $(p_1, p_2)$-plane; however, for the finite ($T = 2^{10}$) run of figure 5(*c*), an open space is discernible between the two families of half-cycles. At values of $\bar{\beta}$ less than about $-0.80$, depending on the initial conditions, the chaotic trajectories comprise a trajectory with a shape resembling that for $\bar{\beta} = -0.70$ (but without the residual period-doubling characteristic) together with its reflection in the $p_2 = 0$ axis, presumably representing a repeated (albeit random) transition between a particular solution and its $(p_1, q_1, p_2, q_2) \rightarrow (p_1, q_1, -p_2, -q_2)$ reflection (see remark following (4.3)). For $\bar{\beta}$ substantially above $-0.80$, e.g. $\bar{\beta} = -0.70$, this transition occurs only rarely and is not captured in a run as long as $2^{11}$; on the other hand, for $\bar{\beta}$ substantially below $-0.80$, e.g. $\bar{\beta} = -0.85$ (figure 5*d*), the transition occurs every few cycles (typically every 1–3 cycles, yielding an almost symmetrical pattern. Chaotic motion remains until $\bar{\beta}$ is decreased to $\bar{\beta} = \bar{\beta}_3 = -1.44$, with fixed-point solutions being obtained for $\bar{\beta} \leqslant -1.44$. It must be emphasized, however, that the sampling interval of $\bar{\beta}$ for this series of runs is rather coarse and that it is possible, or even likely, that

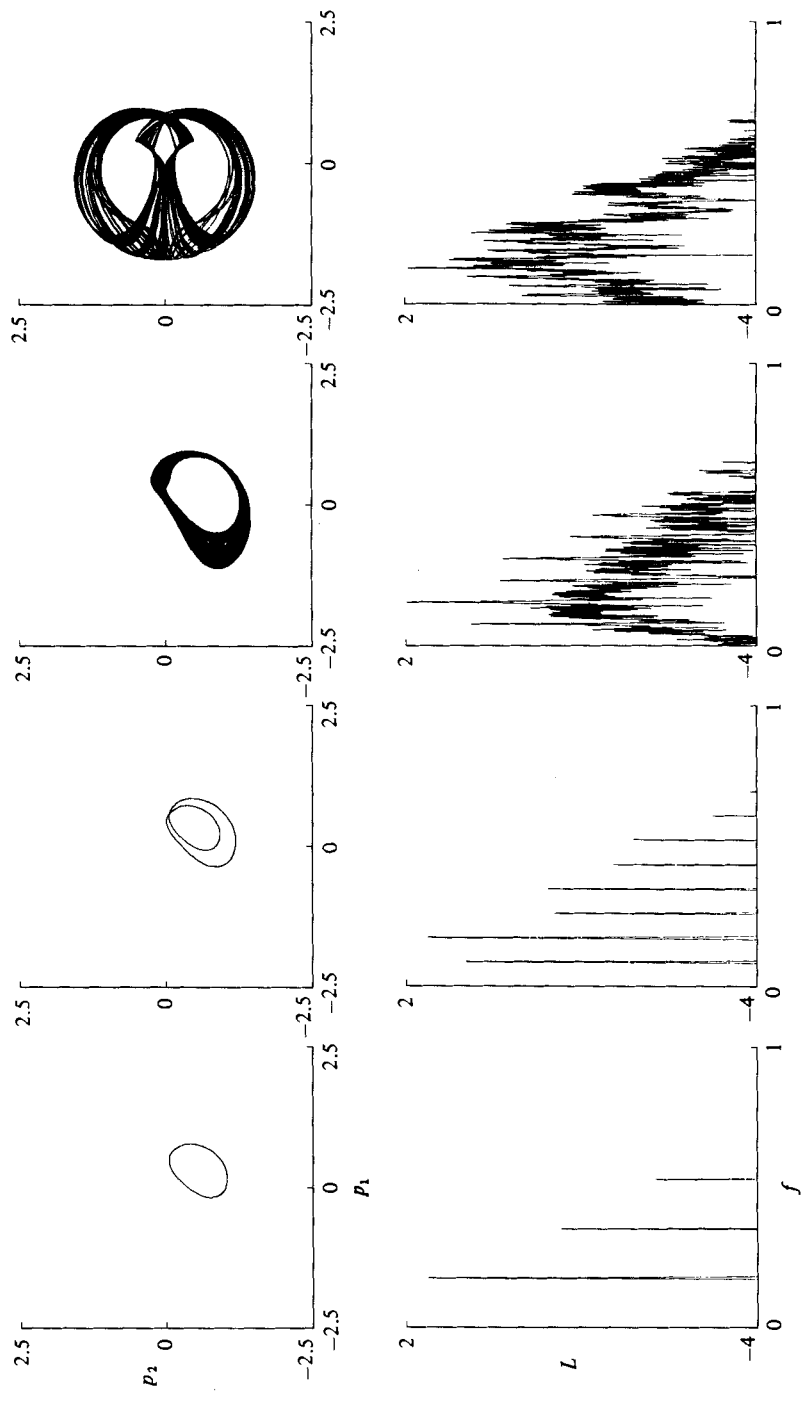


FIGURE 5. Phase-plane $(p_1, p_2)$ projections and power spectra ($L \equiv \log_{10} P$ versus $f$)for $\mu = 1.3772$ ($d/a \to \infty$), $A^{-\frac{1}{3}}\alpha^2 = \frac{1}{8}$, and $\overline{\beta} = -0.52$ (*a*), $-0.54$ (*b*) $-0.70$ (*c*) and $-0.85$ (*d*). The initial conditions are $(p_1, q_1, p_2, q_2) \equiv (0, 0, 0, 1)$. The data for $0 < \tau < 64$ (512 for $\overline{\beta} = -0.54$) are omitted in order to eliminate transients. The zero-frequency component of the power spectrum has been eliminated.

| $A^{-\frac{1}{3}}\beta$ | $\log_2 T$ | Trajectory |
|---|---|---|
| $-1.1$ | 7 | FP |
| $-1.2$ | | LC |
| $-1.3$ | | LC–PD |
| $-1.4$ | | LC |
| $-1.5$ | | Chaotic |
| $-1.6$ | | LC |
| $-1.65$ | 6 | FP |
| $-1.7$ | | FP |
| $-1.8$ | | FP |

TABLE 2. Results of numerical integration for $\mu = 0.6$, $A^{-\frac{2}{3}}\alpha^2 = \frac{1}{8}$

(as in the pendulum problem) there are subintervals within $-0.70 \geqslant \bar{\beta} \geqslant -1.43$ in which limit cycles, rather than chaotic trajectories, are attained.

A second series of runs was made for $\mu = 0.6$ and $\alpha^2 = \frac{1}{8}A^{\frac{2}{3}}$, for which $\bar{\beta}_{2*} = -1.21$ and $\bar{\beta}_3 = -1.44$ (table 2). Limit cycles appear, as expected, as $\bar{\beta}$ is decreased through $\bar{\beta}_{2*}$, and persist, with a brief window of chaotic motions in a small neighbourhood of $\bar{\beta} = -1.5$, down to just below $\bar{\beta} = -1.60$, which is significantly below $\bar{\beta}_3 = -1.44$. A similar extension of the limit-cycle regime below the turning point of the planar resonance curve was observed for the pendulum and appears to represent either a very long transient or, more plausibly, a finite-amplitude extension of the basin of attraction (in the phase space) of the limit-cycle regime.

This work was supported in part by the Physical Oceanography Division, National Science Foundation, NSF Grant OCE-81-17539, and by the Office of Naval Research, Contract NR 062-318 (430).

## Appendix. Comparison with Hutton (1963)

Hutton (1963) considers only a single configuration, for which $a = 5.44$ in., $d = 8.91$ in. ($d/a = \frac{3}{2}$), and $\omega_1 = 10.90$ rad/s. Comparing his formulation with mine, in particular his evolution equation (A 37*b*) with my (4.3*b*), I find that

$$A = 2\left(\frac{\omega}{k^2 x_1}\right)^2 F_1^2 K_1, \quad \mu = \frac{1}{2}\frac{K_2}{K_1}, \tag{A 1$a$, $b$}$$

where $F_1$ is given by his (A 38*a*), and $K_1 = 0.485 \times 10^{-5}$ and $K_2 = 1.371 \times 10^{-5}$ are given by his table 2. The units of $K_1$ and $K_2$, which must be (time)$^2$/(length)$^4$, are not stated; however, all lengths for which dimensions are given are in inches. Taking the units of the above values of $K_1$ and $K_2$ to be s$^2$/in.$^4$, I obtain $A = 1.05$ and $\mu = 1.41$, which are close to the values $A = 1.08$ and $\mu = 1.38$ given by the results in II for $d/a = \frac{3}{2}$. There are significant discrepancies between the values of the various integrals given by Hutton's table 2 and the values in II, but Hutton (private communication) informs me that the correct values of the integrals were used in his calculations of $K_1$ and $K_2$ and that errors in his table 2 were introduced in a subsequent revision of his normalizations.

## REFERENCES

GUREL, O. 1979 Poincaré's bifurcation analysis. *Ann. NY Acad. Sci.* **316**, 5–26.

HUTTON, R. E. 1963 An investigation of resonant, nonlinear, nonplanar, free surface oscillations of a fluid. *NASA Tech. Note* D-1870 (*Washington*).

LICHTENBERG, A. J. & LIEBERMAN, M. A. 1983 *Regular and Stochastic Motion.* Springer.

LORENZ, E. N. 1963 Deterministic nonperiodic flow. *J. Atmos. Sci.* **20**, 130–141.

MILES, J. W. 1962 Stability of forced oscillations of a spherical pendulum. *Q. Appl. Maths* **20**, 21–32.

MILES, J. W. 1976 Nonlinear surface waves in closed basins. *J. Fluid Mech.* **75**, 419–448.

MILES, J. W. 1984*a* Resonant motion of a spherical pendulum. *Physica* **11D**, 309–323.

MILES, J. W. 1984*b* Internally resonant surface waves in a circular cylinder. *J. Fluid Mech.* **149**, 1–14.

MILES, J. W. 1984*c* Resonant non-planar motion of a stretched string. *J. Acoust. Soc. Am.* **75**, 1505–1510.